# Molecular dynamics simulation of synchronization in driven particles

Tiare Guerrero* and Danielle McDermott†

*Department of Physics, Pacific University, Forest Grove, OR 97116*

(Dated: December 30, 2020)

Particles driven across a washboard potential energy landscape exhibit a variety of synchronization effects. We discuss a simple numerical model that provides insight to synchronization behavior using molecular dynamics simulations for particles moving through a viscous liquid. This model reproduces behaviors observed in experimental systems of interest to condensed matter physics including magnetically driven colloidal particles confined by light-fields. We demonstrate how to visualize the system with numerical representations of the landscape and animations of the particle motion. Our results show a variety of synchronization effects in single and multi-particle systems, which we characterize with plots of particle velocity as a function of applied driving force, and phase diagrams of position versus velocity.

## I. INTRODUCTION

Synchronization is a universal phenomena in which individual oscillators adjust frequency due to interaction or an external stimulus [1]. Synchronous behaviors where oscillators move in-phase (i.e. in time) are observed in many everyday systems such as the flickering candle flames coupled by temperature fluctuations [3], vibrations of singing wineglasses [4], and metronomes coupled through a supporting platform [5]. Biological systems benefit from cooperative synchronization such as birds coordinating wing flaps to optimize energy use during flight [6], frogs alternating croaking patterns [7], and humans synchronizing clapping in time with music [8]. At a cellular level, neurons simultaneously fire in cardiac muscle [9] and brain tissue [10].

A particular form of synchronization is phase-locking or mode-locking, which first appeared in the scientific literature with Huygens' 1665 experiments on the motions of two wall-mounted pendulum clocks. Huygens demonstrated the tendency of the pendula to swing in time due to interactions through the wall, no matter the original phase of the clocks [2]. Dynamical systems exhibit phase-locking when oscillators with different rhythms couple so the frequency ratio or mode is an integer number [12]. The phenomena is often studied with simplified computational models and can be visualized with with phase plots or Lissajous figures. A mode-locked system is confined to a closed loop in a parametric space showing the relationship between two periodic functions with patterns determined by the mode, first reported in 1857 [13] and easily generated with a computer code or oscilloscope [14]. (*As we will demonstrate in phase plots in Figs. X, Y, Z*)

External forcing can cause or regulate synchronization. For instance a pacemaker (an electrical generator) pulses to regulate a heart beat or controlling the pattern of flashing fireflies with a pulsed light [15]. These behaviors

can be modeled with numerical studies where a driving force is applied to simple harmonic system, either coupled oscillators or a single particle driven across a periodic potential landscape. A single particle particle oscillator within a potential well is much like a skateboarder in a half-pipe or a child on a swing moving back and forth through equilibrium. Single particle studies are useful to understand synchronization in the absence of collective effects. With a constant or dc drive the landscape modulates the particle velocity, below some threshold below the dc force is not strong enough to push the particle across a potential maximum so the average velocity is zero, a phenomena known as depinning [23], and dissipating energy from the system at all driving forces. A sinusoidal or ac drive creates mode-locking, where the average particle velocity is fixed for a range of dc drive forces [24].

Dynamical mode-locking is observed in quantum electronic devices such as Josephson junctions [16, 17]. A single junction contains two superconductoring layers which sandwich an insulating layer. When subject to an external voltage, Cooper pairs in the superconducting materials tunnel through the insulating layer. Phase-locking is observed as stepped regions in current-voltage (I-V) relationship in these devices, where voltage is the analog of external driving force and current is that of particle velocity. Known as Shapiro steps, these phase locked currents have been observed due to applied ac voltages in single Josephson junctions [19, 21] and coupled arrays of junctions [20]. Shapiro steps vary in width depending on the strength of the applied AC forces, and are observed in a variety of systems displaying non-Ohmic behavior in voltage-current curves, including ac and dc driven charge and spin density waves.

## II. COLLOIDAL MODELS

Complex dynamics can be studied with colloid particles with experiments and simulation. In experiment, colloids are typically spheres of plastic suspended in highly de-ionized water or silica in suspended in organic solvent. The spheres are a few microns in size and move at rates

---

*Electronic address: guer9330@pacificu.edu
†Electronic address: mcdermott@pacific.edu

of microns per second, so a system can be imaged with a traditional optical camera due to the large size and slow speed of the particles. Individual colloids exhibit Brownian motion, where particles change direction in a seemly random fashion due to unseen collisions with particles comprising the suspending fluid []. Brownian motion is a temperature dependent phenomena affecting quantum mechanically small systems. [] [elaborate].

Due to the relative ease of manipulation and imaging, colloids are used as experimental models for systems relatively hard to access and visualize. Collections of colloids can be used to study the properties of solids and liquids or more exotic systems such as cold atoms or electron gases [29]. The interaction forces between colloids can be controlled by altering the chemistry of the suspending fluid or surface ligands of the particles. Thus colloids can be modified to mimic different systems such as hard spheres interacting via contact forces [], dipole interactions [], and long range electrostatic interactions [].

Light is a tool for manipulating the colloidal environment. A single laser beam can be used to create an optical trap, which uses photon radiation pressure to control colloid motions. A circular optical trap is designed so the center is a local energy minimum where a colloid in the beam center is subject to a uniform distribution of photon bombardment. Colloids at a trap edge experience a net force due to the uneven distribution of photon collisions on its surface. Depending on the shape of the trap and location of the particle in the trap, the radiation pressure either pushes colloids toward the local minima or ejects it from the trap. A single optically trapped colloid executing Brownian motion is a useful probe of microscopic forces, and has been studied in detail in Ref. [30].

Complex environments can be engineered with light by using diffraction gratings to create a patterned potential energy landscape with one or more laser beams [].

Experiments of colloid particles confined in optical traps arrays or patterns subject to external driving forces have been used to examine the microscopic dynamics of individual particles during mode-locking [25]. This produced step-by-step diagrams of particle dynamics that cannot be imaged in electronic systems such as Josephson junctions. Thus the study of mode-locking is a useful problem of complex quantum mechanical systems. Mode-locked colloid dynamics have been achieved in experiments [25, 31] and simulations [27, 28] for a variety of interaction types such as magnetic dipoles and electric forces.

Numerical modeling of colloids can provide mechanistic insight that can be difficult to achieve in experimental conditions where Brownian motion and other sources of noise dominate.

Here we perform numerical studies on the synchronized dynamics of confined particles driven over a washboard shaped potential energy landscape. We chose this model for its relevance to condensed matter systems and ease of simulation. The period of the substrate can be used to control the intrinsic velocity of the dc driven particle, and the applied ac drive can create Shapiro steps in the force-velocity relationship.

We describe our molecular dynamics model for a single particle in Section III. We summarize our results including synchronized motion of a single confined particle driven across a periodic landscape in Section IV. In Section IV A we extend the model to include multiple particles, and show how confined interacting particles respond to the same applied driving force. We conclude with exercises for interested students in Section VII.

## III. MOLECULAR DYNAMICS SIMULATION

We use a classical model for studying the dynamics of $N$ interacting particles, using the net force on each particle to calculate its trajectory. Particles are confined in a two-dimensional (2D) simulation of area $A = L \times L$ where $L = 36.5a_0$ where $a_0$ is a dimensionless unit of length. An individual particle $i$ has position $\vec{r}_i = x_i\hat{x} + y_i\hat{y}$ and velocity $\vec{v}_i = d\vec{r}_i/dt$. The edges of the system are treated with periodic boundary conditions such that a particle leaving the edge of the system is mapped back to a position within the simulation by the transformation $x_i + L \to x_i$ and $y_i + L \to y_i$. We show a schematic of the system in Fig. 1(a).

We confine the particles using a position dependent potential energy function, called a landscape or substrate. The confining force is calculated as $\vec{F}_i^l(\vec{r}_i) = -\nabla U_l(\vec{r}_i)$. The landscape is modulated in the y-direction with the periodic function

$$U(y) = U_0 \cos\left(N_p \pi y/L\right) \qquad (1)$$

where $N_p$ are the number of periods, and $U_0$ is an adjustable parameter to set the depth of the minima with simulation units of energy $E_0 = 1$. We plot this function in Fig. 1 we use $N_p = 3$ to illustrate the features of Eq. 1. In Fig. 1(a) we show the $x-y$ plane with a contour plot of the the 2D potential energy landscape, where the maxima are colored red and the minima colored blue. In Fig. 1(b) we plot the function $U(y)$ to illustrate how the magnitude $\vec{F}_i^l$ is calculated from particle position in the $y-$direction.

Particles are subject an external time-dependent driving force $\vec{F}_D(t)$ applied parallel to the y-direction. We model this force as

$$\vec{F}^D(t) = [F^{DC} + F^{AC}\sin(\omega t)]\hat{y}, \qquad (2)$$

with modifiable parameters including a constant component $F^{DC}$, and a time dependent component with amplitude $F^{AC}$ and frequency $\omega = 2\pi f$. We illustrate this force in Fig. 1(a) in the positive $y-$direction. When $F^{DC}$
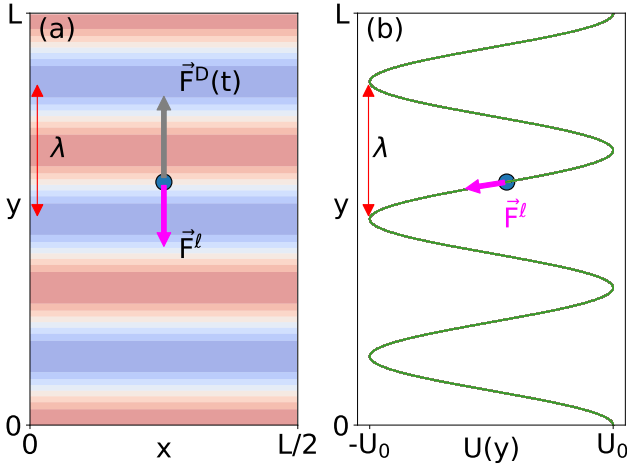
FIG. 1: Schematic of the simulation of a single particle driven across a washboard potential energy landscape. The period of the landscape, $\lambda = L/N_p$ where $N_p = 3$, is marked in red. The force due to the landscape is calculated from the gradient of the potential energy $\vec{F}^l = -\nabla U(\vec{r})$. (a) View of the $x-y$ plane. The time-dependent applied driving force $\vec{F}^D$ is parallel to the y-axis. The landscape is shown with a contour plot, with maxima in the potential energy marked in red and minima marked in blue. A particle is shown in the region between minima and maxima subject to competing forces due to the landscape and applied driving force. (b) The potential energy function along the y-axis $U_l(y)$, The particle in (a) is shown at the same $y-$position, where the magnitude of force $\vec{F}^l$ is calculated as the slope of this function, directed along the $y-$direction in panel (a).

is non-zero, we slowly increase $F^{DC}$ from zero to avoid transient effects.

We model the particle dynamics with an overdamped equation of motion. The term overdamped or critically damped indicates that an oscillator cannot undergo periodic undulations due to some external force. In our colloidal model we assume the damping comes from the viscosity of the fluid, where a sphere of radius $0.5\mu m$ has a Reynolds number of $R \approx 10^{-6}$, indicating that linear drag dominates the particle motion. See Section VII Exercise 1 for more information about the Reynold's number. In the overdamped model the linear friction produced by this nonconservative force, $\vec{F}_{drag} = -\eta\vec{v}_i$ is sufficient so that the acceleration of the particle is zero. Such a model is appropriate when the particles are small and the viscosity of the suspending medium is high.

Newton's second law for an individual particle $m\vec{a}_i = \sum \vec{F}$ is simplified by the assumption $\vec{a}_i$ is zero in overdamped model. The equation of motion for an isolated particle is

$$\eta\vec{v}_i = \vec{F}_i^l + \vec{F}^D(t). \qquad (3)$$

with the viscosity coefficient $\eta = 1$, which we describe in more detail in Exercise 1. In Section VII Exercise 2 we invite the reader to confirm this result.

The equation of motion provides a direct calculation of the velocity of an individual particle from its location $\vec{r}_i$ and the simulation time. The molecular dynamics simulation is controlled by a $for()$ loop which runs from an initial to maximum integer number of time steps $t_i$. Each integer time step interval $t_{i+1} - t_i$ represents a simulation time interval of $\Delta t$ simulation units. At each time step we evaluate the net force on each particle as a function of its position $\vec{r}_i(t)$ and then integrate the equation of motion to move particles to an updated position $\vec{r}_i(t+\Delta t)$. Since the acceleration as zero, the integration of the equation of motion is performed via the Euler method

$$\vec{r}_i(t + \Delta t) = \vec{v}_i(t)\Delta t + \vec{r}_i(t) \qquad (4)$$

for a small time step $\Delta t$. In Section VII Exercise 3 we elaborate on the numerical methods for solving differential equations, and demonstrate how the Verlet method simplifies to the Euler method when $\vec{a} = 0$. The units of the simulated variables are summarized in Table I.

TABLE I: Simulation units.

| Quantity | Unit |
|---|---|
| length | $a_0 = 1$ |
| energy | $E_0 = 1$ |
| force | $E_0/a_0$ |
| viscosity coefficient | $\eta = 1$ |
| velocity | $E_0/(\eta a_0)$ |
| time | $(\eta/E_0)a_0{}^2$ |

## IV. MODE-LOCKING OF A SINGLE PARTICLE

We drive a single particle across a periodic landscape along the y-direction described in Eq. 1 with $N_p = 20$ and landscape period $\lambda = 1.825a_0$. The numerical implementation of the landscape is calculated with

$$F_y^l(y) = -A_p \sin\left(N_p\pi y/L\right) \qquad (5)$$

where the force is scaled with parameter $A_p = 0.1$ in simulation units for force.

In Fig. 2 we show the relationship between the applied force and particle position. In Fig. 2(a) we plot the applied driving force defined in Eq. 2 as a function of time. The time independent constants are $F^{AC} = 0.2$, $F^{DC} = 0.01$, and $f = 0.01$ cycles per time unit. The time period of the driving force is $T = 1/f = 100$, with the initial driving force at is minimum value $F^D(0) = F^{DC}$.

In Fig. 2(b) we show the $y-$position of the particle as a function of time, where we normalize $y$ by the spatial period of the washboard as $y/\lambda$. The initial particle position is $y = 0$, where the landscape force is minimum $F^l = 0$. Subsequent substrate minima are located at integer multiples $y/\lambda = 1/2, 3/2, 5/2$, et cetera.

When $F^D(t) > A_p$, a particle can overcome the barrier height of the landscape troughs, and the particle hops between minima in the energy landscape. In Fig. 2 we demonstrate this relationship, where over half of a driving period ($T = 50$) while $F_D(t) > 0$ the particle moves in the positive y-direction through three substrate troughs, reaching a maximum of $y/\lambda = 3$. When $F_D(t) < 0$ the particle moves in the negative y-direction reaching a minimum position of $y/\lambda = 1$ over the total period $T = 100$. The average velocity $\bar{v}_y$ is the average displacement $\Delta y = y(t_0 + T) - y(t_0)$ over the period of the driving force. In Fig. 2 the average displacement during one time period is a single wavelength of the substrate $y(t_0 + T) - y(t_0) = \lambda$. Thus the average velocity is $\bar{v}_y = \lambda f$.

rate of $\Delta F^{DC} = 0.001$ every $\Delta t = 4000$ integer timesteps or 40 time units. By modifying $F^{DC}$ we achieve a variety of oscillation modes. A mode is a periodic pattern of hops with a constant average particle velocity, $\bar{v}_y$ over a range of driving forces $F^{DC}$. We illustrate mode-locking in the velocity-force plot in Fig. 3(b). Here $\bar{v}_y$ is increasing in non-uniform steps, with a quantized height of $\bar{v}_y = n\lambda f$, where $n$ is an integer, $\lambda = L/N_p = 36.5/20 = 1.825$ is the spatial period, or wavelength of the landscape, and $f = 0.01$ cycles per time unit.

Our simulations reproduce results presented in Juniper et al. [25, 26] which demonstrated mode locking in experiments of driven colloids on a optical periodic landscape.

We illustrate the hopping pattern in Fig. 3(b) and show the dynamics in supplementary materials [37].
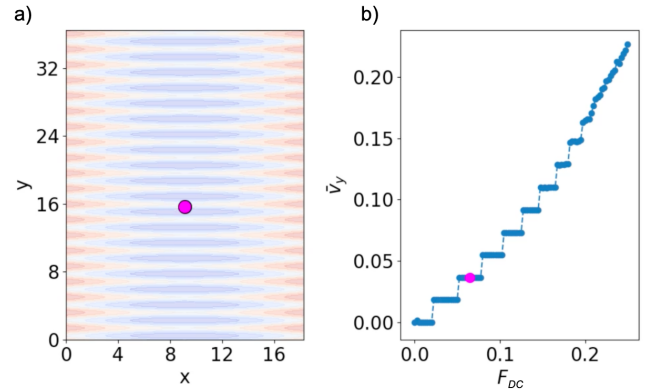


FIG. 3: **(a)** The particle is driven with a constant amplitude $F^{AC}$ and frequency $\omega$ through a periodic spatial potential landscape. The landscape is represented with a colormap where blue are minima and red are maxima in the potential. **(b)** An average particle velocity in the y-direction $\bar{v}_y$ as a function of a constant driving force $F^{DC}$. In the animation available in Ref. [37] the magenta dot represents the average velocity of the particle $\bar{v}_y$ at which the particle in Fig. 1(a) is moving.


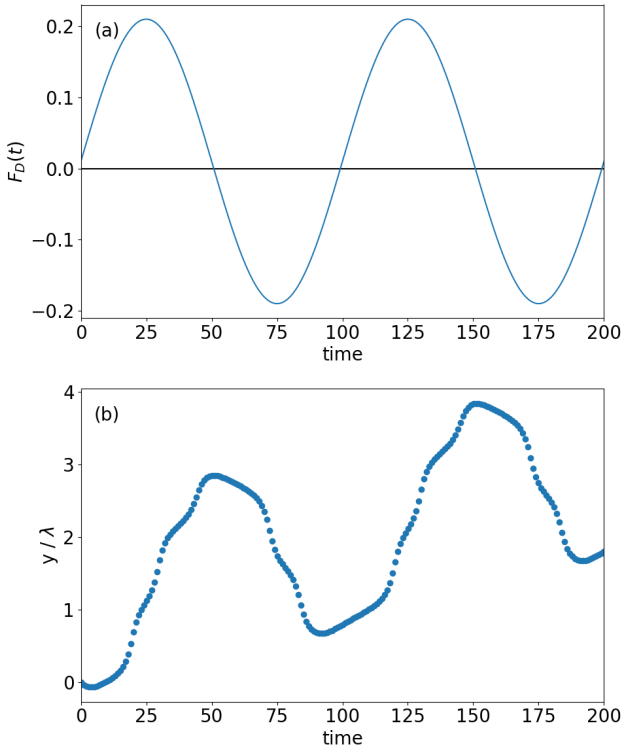
FIG. 2: The position as a function of time of a single driven particle normalized by the period of the substrate $\lambda$.

Phase locked steps occur for average displacements integer multiples of the substrate period $n\lambda$.

We sample the average velocity $\langle v_y \rangle$ as a function of $F^{DC}$.

The hopping pattern of the driven particle is periodic, and could be achieved over a range of $F^{DC}$. We explore the ranges of periodic hopping patterns by increasing $F^{DC}$ as a function of time, as shown in Fig. 3. We apply an external applied force, with a constant $F^{AC}$ with frequency $\omega = 2\pi f$ then slowly increase $F^{DC}$ at a

## A. Synchronization in multi-particle systems

Particles in confined geometries behave differently than free particles. Stabilized charged particles form patterns due to the interplay of the confining landscape and particle interactions. Narrow channels studies are useful to provide insights of how particles move through systems such as charge carries in quantum wires [32] and slime molds in microchannels [33]. In multi-particle simulations, we confine the particles to a narrow region along the $x-$direction using a periodic function

$$U_{q1D}(x) = U_{q0} \cos{(\pi x/L)} \tag{6}$$

where $U_{q0}$ defines the channel depth. This quasi-one-dimensional geometry confines the particles primarily to

move along the y-direction but allows for some lateral motion of particles. Otherwise the repulsive interaction between particles would cause them to spread throughout the system. The total landscape potential energy function is the sum

$$U_{landscape}(x,y) = U_{q1D}(x) + U_{washboard}(y) \qquad (7)$$

We explore collective effects in a twenty particle system confined to a narrow channel, as shown in Fig. 2a). We create the confining channel with a sinusoidal function with a single period.

$$U_l(x) = U_{0x} \cos(\pi x/L). \qquad (8)$$

The landscape potential energy is illustrated in Fig. 4(a) where red regions are high potential and blue regions are low potential.

We model particle interaction forces $\vec{F}_{ij} = -\nabla U_{ij}(r_{ij})$ with the Yukawa potential energy

$$U_{ij}(r_{ij}) = \frac{E_0}{r_{ij}} e^{-\kappa r_{ij}}, \qquad (9)$$

where particle $i$ and $j$ are distance $r_{ij} = |\vec{r}_i - \vec{r}_j|$ apart. This screened Coulomb potential is scaled in terms of energy unit $E_0$ defined in Table I. $\kappa = 1/R_0$ is the screening parameter that describes the length scale at which particles interact. We fix the screening length scale $R_0$ to be $a_0$ (i.e. unity in simulation units). In experiments charge screening is observed due to ions in the suspending fluid and the charges of surrounding particles which reduces the interaction range of individual particles. Because the particles interact over short ranges, the numerical models can be run efficiency using a neighbor list algorithm determined using a cell method. [explain and reference!]

Newton's second law can be rearranged to the equation of motion a single particle subject to collective effects is

$$\eta \vec{v}_i = \vec{F}_i^l + \sum_{i \neq j}^{N} \vec{F}_{ij} + \vec{F}_D(t). \qquad (10)$$

The initial configuration of the system is shown in Fig. 4(a). We annealed the system into a ground-state configuration by raising the system to a high temperature $T$, and slowly lowering the temperature in steps of $dT = -0.01$ until the particles form a buckled chain in the low region of the channel due to the competition between particle repulsion and channel confinement. The interparticle forces between neighboring particles cause the system to form a buckled chain. The molecular dynamics of simulated annealing is described in Ref. **??**. Once the ground state particle configuration is obtained, no further annealing is necessary, so the our simulations begin with particle configurations that result from the annealing process, as listed in Appendix [ref] and available in supplementary material.

When a single particle is driven, the neighboring particles act similarly to a periodic landscape to impede its motion. A driven particle can exhibit mode locking with a well-chosen AC drive and frequency. In the attached movie, Figure2.mp4, we show the complex dynamics of mode locking, where the driven particle leap-frogs past the other particles.
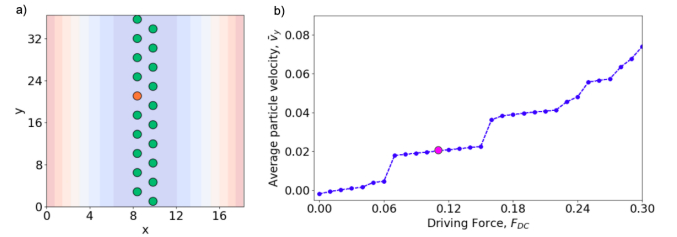


FIG. 4: **(a)** A single particle (colored orange - mark in some manner for non-color views) is driven with a constant amplitude $F^{AC}$ and frequency $\omega$ through 19 neighboring particles (colored green - mark differently) confined by a quasi one-dimensional channel. The landscape is colored as in Fig. **??**(a). **(b)** Average $\bar{v}_y$ versus $F^{DC}$, where $\bar{v}_y$ is the average particle velocity of the driven particle in the y-direction.

### B. Kinked system

We confine $N$ particles to $N-1$ troughs to create a local high density region. $F^{DC}/F^{AC} = 1$ [CHECK!]

## V. QUASI-PERIODIC SUBSTRATE

## VI. CHAOTIC DYNAMICS

## VII. ASSOCIATED PROBLEMS

1. Stokes' law the viscous drag on a sphere is $\vec{F}_{lin} = 3\pi \eta D \vec{v}$ [] where the fluid viscosity is $\eta$, $D$ is the particle diameter. Assuming a colloid with diameter $D = 1\mu m$ and the viscosity of water at room temperature is $\eta = 0.01 cm^2/sec$ [] Reynold's number $R = Dv\rho/\eta$ where $\rho$ is the fluid density and $v$ the particle's speed. When $R$ is small, the quadratic and higher order drag terms may be ignored in favor of the linear drag term. A velocity $v$ in experiment is on the order of $v \sim 1\mu/s$, thus $R \approx 10^-6$.

   This model should be familiar to readers of a standard classical mechanics text, such as Ref. [36] when studying models Millikan's oil drops.

2. Newton's second law states that the sum of forces on a particle is proportional to the acceleration of the particle.

$$m\vec{a}_i = \sum \vec{F} \qquad (11)$$

Demonstrate that Eq. 10 is obtained from Newton's second law.

3. Generally when solving differential equations, the Euler method is effective for solving linear equations, such as the one-dimensional $f(y) = df/dy$ but not higher order methods.

   The Verlet method simplifies to

   Because we are performing molecular dynamics for a single particle on a smooth potential energy landscape, we use a large simulation time step of $\Delta t = 0.01$. In Sec. IV A, we decrease the time step to treat multiple particle interactions.

4. Drawing the contour

   The code for generating a two dimensional colored plot of the potential landscape is calculated by evaluating the analytic function in Eq. **??** for a grid of values $(x_n, y_n)$.

5. Kuramoto model = overdamped interacting rotors/oscillators are used to model coupled oscillator systems - no substrate or external drive so far as I can see - this seems baked into the oscillator properties/interactions

6. Brownian motion without fluid dynamics using Ermak's algorithm

7. Frenkel-Kontorova and competing length scales for low temperature systems where thermal fluctuations are negligible

8. The Fokker-Planck Equation

9. Aubrey-Kontorova + commensurability

10. nanotribology

    kink motion Vanossi et al J.Phys.: Condens. Matter 19 (2007)

## VIII.   CONCLUSION

## IX.   SUPPLEMENTARY MATERIALS

### A.   Grid Contour Plot of landscape

Testing section - how will putting the code directly in the appendix appear?

```
##############################################
#ADD CONTOUR PLOT
##############################################
def add_contour(ax,L,N,corrugated = True):
```

```
'''
Hardwired to color quasi1D potential
that contains
the particles in a trough.
Can add the washboard/corrugated substrate.

Required Arguments

Optional Arguments:

corrugated (default = True)
Adds the washboard in the y-direction.
Hardwired for a single parameter set.
'''

a_p = L/N

#we don't want to cover the entire range
X = np.arange(0, L/2.0, 0.1)
Y = np.arange(0, L, 0.1)
X, Y = np.meshgrid(X, Y)

Z_mag = 2.0 # set by what "looks good"
Z = Z_mag*np.sin(2*np.pi*X/L)
if corrugated == True:
    Z += np.sin(2*np.pi*(Y+1.75)/a_p)

cmap=cm.coolwarm_r

#alpha = transparency. set by what looks good.
cset = ax.contourf(X,Y,Z,cmap=cmap,alpha=0.25)

#ax1.set_xlim(15,20)
#ax1.set_ylim(15,20)

#ax1.set_xlabel(r"$X$")
#ax1.set_ylabel(r"$y$",rotation='horizontal',ha=':

#ax1.set_xticks([])
#ax1.set_yticks([])
return
```

[1] A. Pikovsky, M. Rosenblum, and J. Kurths, *Synchronization: A Universal Concept in Nonlinear Sciences* (Cambridge Univ. Press, Cambridge, 2003).

[2] M. Bennett, M.F. Schatz, H. Rockwood, and K. Wiesenfeld, Huygens' clocks, Proc. Roy. Soc. A **458**, 563 (2002).

[3] K. Okamoto, A. Kijima, Y. Umeno, and H. Shima. Synchronization in flickering of three-coupled candle flames. Sci Rep **6**, 36145 (2016)

[4] T. Arane, A. K. R. Musalem and M. Fridman, Coupling between two singing wineglasses, Am. J. Phys. **77**, 1066 (2009).

[5] J. Jia, Z. Song, W. Liu, J. Kurths, and Xiao, J. Experimental study of the triplet synchronization of coupled nonidentical mechanical metronomes. Sci. Rep. **5**, 17008 (2015).

[6] S. Portugal, T. Hubel, J. Fritz, S. Heese, D. Trobe, B. Voelkl, S. Hailes, A. M. Wilson and J. R. Usherwood. Upwash exploitation and downwash avoidance by flap phasing in ibis formation flight. Nature **505**, 399 (2014).

[7] I. Aihara, T. Mizumoto, T. Otsuka, H. Awano, K. Nagira, H. G. Okuno and K. Aihara. Spatio-Temporal Dynamics in Collective Frog Choruses Examined by Mathematical Modeling and Field Observations. Sci Rep **4**, 3891 (2014).

[8] P. Tranchant, D. T. Vuvan, and I. Peretz, Keeping the Beat: A Large Sample Study of Bouncing and Clapping to Music. PLoS ONE 11(7): e0160178. (2016).

[9] G. Martin Hall, Sonya Bahar, and Daniel J. Gauthier, Prevalence of Rate-Dependent Behaviors in Cardiac Muscle. Phys. Rev. Lett. **82**, 2995 (1999).

[10] W. Singer. Striving for coherence. Nature, **397** 391, 1999.

[11] Dutta, S., Parihar, A., Khanna, A. et al. Programmable coupled oscillators for synchronized locomotion. Nat Commun **10**, 3299 (2019).

[12] P. Bak. The Devil's Staircase. Physics Today **39**, 12, 38 (1986).

[13] J. A. Lissajous. "Mmoire sur l'Etude optique des mouvements vibratoires," Annales de chimie et de physique, 3rd series, 51 (1857) 147-232

[14] E. Y. C. Tong, Lissajous figures, The Physics Teacher **35**, 491 (1997).

[15] D. K. Agrawal, J. Woodhouse, and A. A. Seshia, Physical Review Letters **111**, 084101 (2013).

[16] B. D. Josephson, Phys. Letters **16**, 25 (1962).

[17] B. D. Josephson, Advan. Phys. **14**, 419 (1965).

[18] W. C. Stewart CURRENTVOLTAGE CHARACTERISTICS OF JOSEPHSON JUNCTIONS Appl. Phys. Lett. 12, 277 (1968).

[19] S. Shapiro, Josephson currents in superconducting tunneling: the effect of microwaves and other observations, Phys. Rev. Lett. 11, 80 (1963).

[20] S. P. Benz, M. S. Rzchowski, M. Tinkham, and C. J. Lobb, Fractional giant Shapiro steps and spatially correlated phase motion in 2D Josephson arrays, Phys. Rev. Lett. 64, 693 (1990); D. Domnguez and J. V. Jose, Giant Shapiro steps with screening currents, Phys. Rev. Lett. 69, 514 (1992).

[21] A. A. Golubov, M. Yu. Kupriyanov, and E. Ilichev. The current-phase relation in Josephson junctions, Rev. Mod. Phys. **76**, 411 (2004).
quote: Phase engineering techniques are used to control the dynamics of long-bosonic Josephson-junction arrays built by linearly coupling Bose-Einstein condensates.

[22] Dengling Zhang, Haibo Qiu, and Antonio Muoz Mateo, Unlocked-relative-phase states in arrays of Bose-Einstein condensates, Phys. Rev. A **101**, 063623 (2020).

[23] C. Reichhardt and C. J. Olson Reichhardt, Depinning and nonequilibrium dynamic phases of particle assemblies driven over random and ordered substrates: a review, Rep. Prog. Phys. 80, 026501 (2017).

[24] C. Reichhardt, and C. J. O. Reichhardt, Shapiro steps for skyrmion motion on a washboard potential with longitudinal and transverse ac drives. Phys. Rev. B **92**, (22). (2015).

[25] M. P. N. Juniper, A. V. Straube, R. Besseling, D. G. A. L. Aarts, and R. P. A. Dullens, Microscopic dynamics of synchronization in driven colloids. Nat. Commun. 6, 7187 (2015).

[26] Juniper, M. P. N., Zimmermann, U., Straube, A. V., Besseling, R., Aarts, D. G. A. L., Lwen, H., and Dullens, R. P. A. Dynamic mode locking in a driven colloidal system: Experiments and theory. New Journal of Physics, 19(1). (2017).

[27] S. Herrera-Velarde and R. Castaeda-Priego, Superparamagnetic colloids confined in narrow corrugated substrates, Phys. Rev. E **77**, 041407 (2008).

[28] S. Herrera-Velarde and R. Castaeda-Priego, J. Phys.: Condens. Matter 19, 226215 (2007).

[29] D. G. Grier, A revolution in optical manipulation. Nature **424**, 810 (2003).

[30] G. Volpe and G. Volpe, Simulation of a Brownian particle in an optical trap, Am. J. Phys. 81 (3), March 2013

[31] C. Lutz, M. Kollmann, and C. Bechinger, Phys. Rev. Lett. **93**, 026001 (2004); C. Lutz, M. Kollmann, C. Bechinger, and P. Leiderer, J. Phys.: Condens. Matter **16**, S4075 (2004).

[32] S. Tarucha, T. Honda, T. Saku, Solid State Commun. 1995, 94, 413.

[33] A. Gholami, O. Steinbock, V. Zykov, and E. Bodenschatz, Flow-Driven Waves and Phase-Locked Self-Organization in Quasi-One-Dimensional Colonies of Dictyostelium discoideum, Phys. Rev. Lett. **114**, 018103 (2015).

[34] D. Frenkel and B. Smit, Understanding Molecular Simulation: From Algorithms to Applications (Academic Press, London, 2001).

[35] M. P. Allen and D. J. Tildesley, Computer Simulation of Liquids. Second Edition. Oxford University Press (2017).

[36] J. Taylor, Classical mechanics. University Science Books (2005).

[37] See Figure1.mp4 in appropriate